Performance of Normal Geometrical Hydrodynamic Inclined Fixed Pad Thrust Slider Bearing with the Interfacial Slippage Occurring on the Stationary Surface in the Inlet Zone and on the Whole Moving Surface

Yansun Zhou, Yongbin Zhang*, Xuedong Jiang and Mingjun Pang

College of Mechanical Engineering, Changzhou University, Changzhou, Jiangsu Province, China

Abstract: An anaysis is presented for investigating the performance of the hydrodynamic inclined fixed pad thrust slider bearing with a normal geometry where the interfacial slippage occurs on the stationary surface in the inlet zone and on the whole moving surface, based on the limiting interfacial shear strength model. The calculation results show that compared with the classical mode of the bearing (without any interfacial slippage), this bearing has a significantly higher load-carrying capacity but a much lower friction coefficient in the same operating condition. The study shows the considerable improvement of the bearing performance by the introduced interfacial slippage.

Keywords: Bearing, Friction coefficient, Hydrodynamic lubrication, Interfacial slippage, Load.

1. INTRODUCTION

The energy-conserved bearings have been a hot reseearch topic [1-4]. They can prolong the longetivity and improve the operation of machines. It is worth mentioning that the wasted energy would lead to pollution, thus studying the energy-conserved bearings can also protect the environment of human beings.

Low friction is the purpose of energy-converved hydrodynamic bearings. It can be realized by using low-viscosity lubricants [5] and/or adding lubricant additives [6]. In recent years, there were the attempts to artificially introduce the interfacial slippage for improving the overall performance of hydrodynamic bearings including reducing the friction coefficient of the bearings [7-10]. The interfaical slippage technology was suggested as an effective method for develpoing energy-conserved hydrodynamic bearings [11, 12].

The interfacial slippage was ever used to improve the peformance of a normal-geometrical hydrodynamic bearing by being artificially designed on the stationary surface in the beairng inlet zone [7-10]. It can also be used for developing abnormal-geometrical hydrodynamic bearings with certain load-carrying capacities [13-16]; These bearings may have parallel coupled surfaces [13,14], or have divergent surface separations [15, 16], which is objected by classical hydrodnamic lubrication theory.

In the condition of heavy loads and high sliding speeds, we may have difficulty in preventing the interfacial slippage on other bearing surfaces because of the magnitude of the generated shear stress greater than the endurable capacity of the fluid-bearing surface interface. It is questioned that whether there are other modes of energy-conserved hydrodynamic thrust slider bearings which allows the interfacial slippage occurrence on some bearing surfaces. Undoubtedly, such bearings will be more easily realized. There have been the attempts to improve the performance of normal-geometrical hydrodynamic thrust slider beairngs by artificially designing the interfacial slippage on the whole stationary surface [17, 18] or on the whole moving surface [19]. The former kind of the bearings were found to be overall better than the classical mode of the bearings in both the load-carrying capacity and the friction coefficient [17, 18], however the latter kind of the bearing was only better owing to its lower friction coefficient (but with a much smaller load-carrying capacity) [19]. Xia and Zhang [20] developed a new mode of energy-conserved hydrodynamic wedge-platform thrust slider bearing with normal goemetrical configuration by artificially designing the interfacial slippage on both the stationary surface in the bearing inlet zone and the whole moving surface. They showed that this mode of the bearing is overall better than the classical mode of the bearing because of the much higher load-carrying capacity and the much lower friction coefficient.

In this paper, the new mode of energy-conserved hydrodynamic inclined fixed pad thrust slider bearing with normal geometry is proposed by designing the interfacial slippage on both the stationary surface in the

Address correspondence to this article at the College of Mechanical Engineering, Changzhou University, Changzhou, Jiangsu Province, China; Tel: +86 131 9678 5129; E-mail: engmech1@sina.com

E-ISSN: 2409-9848/20

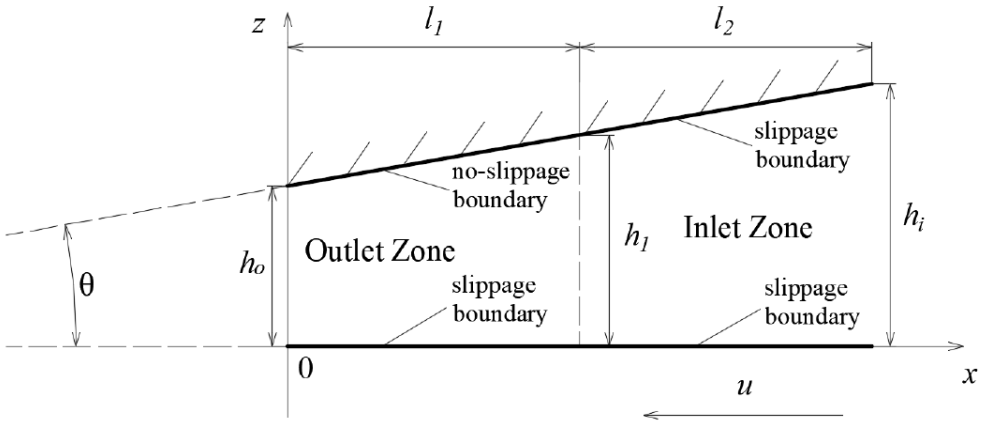

Figure 1: The studied hydrodynamic inclined fixed pad thrust slider bearing with the designed interfacial slippage.

bearing inlet zone and the whole moving surface. The analysis for this bearing has been derived. The carried load and friction coefficient of this bearing were calculated and compared with the classical mode of the bearing (without any interfacial slippage) for the same operating conditions. Conclusions were drawn regarding this excellent mode of hydrodynamic bearing for energy conservation, which is optimistic for actual application.

2. BEARING CONFIGURATION

Figure **1** shows the studied bearing, where the upper contact surface is stationary and the lower contact surface is moving with the speed u. The bearing geometrical configuration is normal. The interfacial slippage occurs both on the stationary surface in the bearing inlet zone and on the whole moving surface owing to the hydrophobicity of these surfaces, but it is absent on the stationary surface in the bearing outlet zone owing to the hydrophilicity of this surface. The widths of the outlet and inlet zones of the bearing are respectively l_1 and l_2, the film thicknesses on the entrance and exit of the bearing are respectively h_i and h_o, the lubricating film thickness on the boundary between the inlet zone and the outlet zone is h_1, and the tilting angle of the bearing is θ. The used coordinates are also shown in Figure **1**.

3. ANALYSIS

The analysis for the bearing in Figure **1** is based on the limiting interfacial shear strength model [21-23], which interprets the interfacial slippage as the result of the interfacial shear stress exceeding the interfacial shear strength. Under low film pressures in a slider bearing, the contact-fluid interfacial shear strength is usually low and can be taken as independent on the film pressure [24-27].

The analysis is based on the following assumptions:

(a) The fluid is isoviscous;

(b) The fluid is incompressible;

(c) The fluid inertia is negligible;

(d) The fluid is in laminar flow;

(e) The condition is isothermal.

3.1. For the Inlet Zone

For a Newtonian fluid, the rheological model is:

$$\tau = \eta \frac{\partial u_x}{\partial z} \tag{1}$$

where τ is the shear stress, η is the fluid dynamic viscosity, u_x is the fluid film velocity in the *x* coordinate direction, and *z* is the coordinate across the film thickness as shown in Figure **1**.

The momentum equilibrium equation for an infinitesimal film element is:

$$\frac{\partial p}{\partial x} = \frac{\partial \tau}{\partial z} \tag{2}$$

where p is the film pressure.

Integrating Eq.(2) gives that:

$$\tau = \frac{\partial p}{\partial x} z + c_1 \tag{3}$$

where c_1 is an integral constant.

Based on the boundary conditions $\tau|_{z=0} = \tau_{sb}$ and $\tau|_{z=h} = \tau_{sa}$, it is solved that $c_1 = \tau_{sb}$; Here, $p|_{x=x_2} = 0$ is the

fluid-contact interfacial shear strength on the stationary surface in the inlet zone and τ_{sb} is the fluid-contact interfacial shear strength on the moving surface. Thus, it is obtained from Eq. (3) that:

$$\frac{\partial p}{\partial x} = \frac{\tau_{sa} - \tau_{sb}}{h} \tag{4}$$

where h is the fluid film thickness.

Integrating Eq. (4) gives that:

$$p = \frac{\tau_{sa} - \tau_{sb}}{k} \ln h + c_2 \tag{5}$$

where $k = \tan(\theta)$ and c_2 is an integral constant.

From the boundary condition $p\big|_{h=h_i} = 0$, it is solved that $c_2 = (\tau_{sb} - \tau_{sa}) \ln h_i / k$. Then the film pressure in the inlet zone is:

$$p = \frac{\tau_{sa} - \tau_{sb}}{k} \ln \frac{h}{h_i} \tag{6}$$

At $h = h_1$, the film pressure is:

$$p_1 = \frac{\tau_{sa} - \tau_{sb}}{k} \ln \frac{h_1}{h_i} \tag{7}$$

3.2. For the Outlet Zone

Substituting Eq.(1) into Eq.(2) gives that:

$$\frac{\partial p}{\partial x} = \eta \frac{\partial^2 u_x}{\partial z^2} \tag{8}$$

Integrating Eq.(8) gives that:

$$u_x = \frac{z^2}{2\eta} \frac{\partial p}{\partial x} + \frac{c_1}{\eta} z + \frac{c_3}{\eta} \tag{9}$$

where c_3 is an integral constant. By substituting Eq.(9) into Eq.(1) and according to the boundary condition $\tau\big|_{z=0} = \tau_{sb}$ and $u_x\big|_{z=h} = 0$, it is resulting that $c_3 = \left(-h^2/2\right)\left(\partial p/\partial x\right) - h\tau_{sb}$. Substituting the results of c_1 and c_3 into Eq. (9) and rearranging gives that:

$$u_x = \frac{z^2 - h^2}{2\eta} \frac{\partial p}{\partial x} + \frac{\tau_{sb}}{\eta}(z - h) \tag{10}$$

The volume flow rate per unit contact length through the bearing is:

$$q_v = \int_0^h u_x \, dz = -\frac{h^3}{3\eta} \frac{\partial p}{\partial x} - \frac{\tau_{sb} h^2}{2\eta} \tag{11}$$

The Reynolds equation for the outlet zone is thus:

$$\frac{\partial p}{\partial x} = -\frac{3\eta q_v}{h^3} - \frac{3\tau_{sb}}{2h} \tag{12}$$

Integrating Eq. (12) gives that:

$$p = \frac{3}{2k}\left(\frac{\eta q_v}{h^2} - \tau_{sb} \ln h\right) + c_4 \tag{13}$$

where c_4 is an integral constant. From the boundary condition $p\big|_{h=h_o} = 0$, it is solved that $c_4 = -3(q_v \eta / h_o^2 + \tau_{sb} \ln h_o)/(2k)$. Then the fluid film pressure in the outlet zone is:

$$p = \frac{3}{2k}\left[q_v \eta \left(\frac{1}{h^2} - \frac{1}{h_o^{\,2}}\right) + \tau_{sb} \ln \frac{h_o}{h}\right] \tag{14}$$

At $h = h_1$, the film pressure is:

$$p_1 = \frac{3}{2k}\left[q_v \eta \left(\frac{1}{h_1^2} - \frac{1}{h_o^{\,2}}\right) + \tau_{sb} \ln \frac{h_o}{h_1}\right] \tag{15}$$

3.3. Volume Flow Rate and Carried Load of the Bearing

Solving the coupled equations (7) and (15) gives the volume flow rate per unit contact length through the bearing as follows:

$$q_v = \frac{\frac{2}{3}(\tau_{sa} - \tau_{sb}) \ln \frac{h_1}{h_i} - \tau_{sb} \ln \frac{h_o}{h_1}}{\eta\left(\frac{1}{h_1^2} - \frac{1}{h_o^{\,2}}\right)} \tag{16}$$

The load per unit contact length carried by the bearing is:

$$\begin{aligned} w &= \int_0^{l_1} p \, dx + \int_{l_1}^{l_1 + l_2} p \, dx \\ &= \frac{3}{2k^2}\left[q_v \eta \left(\frac{2}{h_o} - \frac{1}{h_1} - \frac{h_1}{h_o^2}\right) + \tau_{sb}\left(h_1 \ln \frac{h_o}{h_1} + h_1 - h_o\right)\right] \\ &\quad + \frac{1}{k^2}(\tau_{sa} - \tau_{sb})\left(h_1 - h_i + h_1 \ln \frac{h_i}{h_1}\right) \end{aligned} \tag{17}$$

where on the right-hand side the first integration is for finding the load component in the bearing outlet zone and the second integration is for finding the load component in the bearing inlet zone.

3.4. Shear Stress, Friction Coefficient and Film Slipping Velocity

The shear stress on the upper contact surface in the inlet zone is:

$$\tau_{a,i} = \tau_{sa} \tag{18}$$

The shear stress at the lower contact surface in the inlet zone is:

$$\tau_{b,i} = \tau_{sb} \tag{19}$$

The shear stress at the upper contact surface in the outlet zone is:

$$\tau_{a,o} = -\frac{\tau_{sb}}{2} - \frac{3q_v\eta}{h^2} \tag{20}$$

The shear stress at the lower contact surface in the outlet zone is:

$$\tau_{b,o} = \tau_{sb} \tag{21}$$

The friction force per unit contact length at the upper contact surface in the bearing is:

$$\begin{aligned} F_{f,a} &= \int_0^{l_1} \tau_{a,o}dx + \int_{l_1}^{l_1+l_2} \tau_{a,i}dx \\ &= \frac{1}{k}\left[3q_v\eta\left(\frac{1}{h_1} - \frac{1}{h_o}\right) + \tau_{sa}\left(h_i - h_1\right) + \frac{\tau_{sb}}{2}\left(h_o - h_1\right)\right] \end{aligned} \tag{22}$$

The friction force per unit contact length at the lower contact surface in the bearing is:

$$F_{f,b} = \int_0^{l_1} \tau_{b,o}dx + \int_{l_1}^{l_1+l_2} \tau_{b,i}dx = \frac{\tau_{sb}\left(h_i - h_o\right)}{k} \tag{23}$$

The friction coefficients at the upper and lower contact surfaces in the bearing are respectively:

$$f_a = \frac{\left|F_{f,a}\right|}{w} \quad , \quad f_b = \frac{\left|F_{f,b}\right|}{w} \tag{24}$$

The film slipping velocity on the upper contact surface in the inlet zone is [21]:

$$\Delta u_{a,i} = \frac{q_v}{h} + \frac{\left(2\tau_{sa} + \tau_{sb}\right)h}{6\eta} \tag{25}$$

For ensuring the occurrence of the film slippage on the upper contact surface, it should be satisfied that[21]:

$$\Delta u_{a,i} < 0 \tag{26}$$

Substituting Eq.(25) into Eq.(26) and rearranging finally gives that:

$$\lambda_\tau > \frac{4\ln\frac{H_i}{H_1} + 2\left(H^2 - \frac{H^2}{H_1^2}\right)}{4\ln H_i + 2\ln H_1 + \left(\frac{H^2}{H_1^2} - H^2\right)} \tag{27}$$

where $\lambda_\tau = \tau_{sb}/\tau_{sa}$, $H_1 = h_1/h_o$, $H_i = h_i/h_o$, and $H = h/h_o$.

The film slipping velocity on the lower contact surface in the inlet zone is:

$$\Delta u_{b,i} = \frac{q_v}{h} - \frac{\left(\tau_{sa} + 2\tau_{sb}\right)h}{6\eta} + u \tag{28}$$

where *u* is positive. For ensuring the occurrence of the film slippage on the lower contact surface in the inlet zone, it should be satisfied that [21]:

$$\Delta u_{b,i} > 0 \tag{29}$$

Substituting Eq.(28) into Eq.(29) and rearranging finally gives that:

$$\lambda_\tau < \frac{\frac{6}{\overline{\tau}_{sa}}\left(H - \frac{H}{H_1^2}\right) + 4\ln\frac{H_i}{H_1} - \left(H^2 - \frac{H^2}{H_1^2}\right)}{4\ln H_i + 2\ln H_1 + 2\left(H^2 - \frac{H^2}{H_1^2}\right)} \tag{30}$$

where $\overline{\tau}_{sa} = \tau_{sa}h_o/\left(u\eta\right)$.

The film slipping velocity at the lower contact surface in the outlet zone which is in the *x* coordinate direction is finally:

$$\Delta u_{b,o} = \frac{3q_v}{2h} - \frac{\tau_{sb}h}{4\eta} + u \tag{31}$$

For ensuring the occurrence of the film slippage on the lower contact surface in the outlet zone, it should be satisfied that [21]:

$$\Delta u_{b,o} > 0 \tag{32}$$

Substituting Eq.(31) into Eq.(32) and rearranging finally gives that:

$$\lambda_\tau < \frac{\frac{4}{\overline{\tau}_{sa}}\left(H - \frac{H}{H_1^2}\right) + 4\ln\frac{H_i}{H_1}}{4\ln H_i + 2\ln H_1 + H^2 - \frac{H^2}{H_1^2}} \tag{33}$$

According to Eqs.(27), (30) and (33), it should be satisfied that:

$$\frac{4\ln\frac{H_i}{H_1}+2\left(H_1^2-1\right)}{4\ln H_i+2\ln H_1+1-H_1^2}<\lambda_\tau<\frac{\frac{4}{\overline{\tau}_{sa}}\left(1-\frac{1}{H_1^2}\right)+4\ln\frac{H_i}{H_1}}{4\ln H_i+2\ln H_1+1-\frac{1}{H_1^2}} \quad (34)$$

4. NORMALIZATION

For generality, the following dimensionless parameters are defined:

$$W=\frac{w}{u\eta}\ ,\ P=\frac{ph_o}{u\eta}\ ,\ Q_v=\frac{q_v}{uh_o}\ ,\ \overline{\tau}_{sa}=\frac{\tau_{sa}h_o}{u\eta}\ ,\ \overline{\tau}_{sb}=\frac{\tau_{sb}h_o}{u\eta}$$
$$,\ \overline{\tau}=\frac{\tau h_o}{u\eta}\ ,\ \overline{F}_{f,a}=\frac{F_{f,a}}{u\eta}\ ,\ \overline{F}_{f,b}=\frac{F_{f,b}}{u\eta}\ ,\ Du=\frac{\Delta u_a}{u}\ ,$$
$$X=\frac{x}{l_1+l_2}\ ,\ \psi=\frac{l_1}{l_2}\ ,\ H=\frac{h}{h_o}\ ,\ H_i=\frac{h_i}{h_o}\ ,\ H_1=\frac{h_1}{h_o}\ ,$$
$$\alpha=\frac{h_o}{l_1+l_2}$$

where u is positive.

4.1. For the Present Bearing

The dimensionless volume flow rate per unit contact length through the bearing is:

$$Q_v=\frac{\frac{2}{3}(\overline{\tau}_{sa}-\overline{\tau}_{sb})\ln\frac{H_1}{H_i}+\overline{\tau}_{sb}\ln H_1}{\left(\frac{1}{H_1^2}-1\right)} \quad (35)$$

The dimensionless film pressure in the inlet zone is:

$$P=\frac{\overline{\tau}_{sb}-\overline{\tau}_{sa}}{k}\ln\frac{H_i}{H} \quad (36)$$

The dimensionless film pressure in the outlet zone is:

$$P=\frac{3}{2k}\left[Q_v\left(\frac{1}{H^2}-1\right)-\overline{\tau}_{sb}\ln H\right] \quad (37)$$

The dimensionless load per unit contact length carried by the bearing is:

$$W=\frac{3}{2k^2}[Q_v\left(2-\frac{1}{H_1}-H_1\right)+\overline{\tau}_{sb}\left(H_1-H_1\ln H_1-1\right)]$$
$$+\frac{\left(\overline{\tau}_{sa}-\overline{\tau}_{sb}\right)}{k^2}\left(H_1-H_i+H_1\ln\frac{H_i}{H_1}\right) \quad (38)$$

The dimensionless friction force per unit contact length at the upper contact surface in the bearing is:

$$\overline{F}_{f,a}=\frac{1}{k}\left[3Q_v\left(\frac{1}{H_1}-1\right)+\overline{\tau}_{sa}\left(H_i-H_1\right)+\frac{\overline{\tau}_{sb}}{2}\left(1-H_1\right)\right] \quad (39)$$

The dimensionless friction force per unit contact length at the lower contact surface in the bearing is:

$$\overline{F}_{f,b}=\frac{\overline{\tau}_{sb}\left(H_i-1\right)}{k} \quad (40)$$

The friction coefficients at the upper and lower contact surfaces in the bearing are respectively:

$$f_a=\frac{\left|\overline{F}_{f,a}\right|}{W}\ ,\ f_b=\frac{\left|\overline{F}_{f,b}\right|}{W} \quad (41)$$

4.2. For the Conventional Hydrodynamic Inclined Fixed Pad Thrust Slider Bearing

For comparison, the results for the conventional hydrodynamic inclined fixed pad thrust slider bearing, where is assumed no interfacial slippage, are presented in this section.

The dimensionless volume flow rate per unit contact length through the conventional bearing is:

$$Q_{v,conv}=-H_i/(H_i+1) \quad (42)$$

where $H_i=1+k/\alpha$

The dimensionless hydrodynamic pressure in the inlet zone in the conventional bearing is [28]:

$$P_{conv}=\frac{k}{6}\left(\frac{1}{H}-\frac{1}{H_i}+Q_{v,conv}\left(\frac{1}{H^2}-\frac{1}{H_i^2}\right)\right) \quad (43)$$

where $H=1+kX/\alpha$

The dimensionless load per unit contact length carried by the conventional bearing is [28]:

$$W_{conv}=\frac{6}{k^2}\left(\ln H_i+\frac{H_1}{H_i}-H_1+Q_{v,conv}\left(2-\frac{2}{H_i}+\frac{H_1}{H_i^2}-H_1\right)\right) \quad (44)$$

The dimensionless friction force per unit contact length on the stationary surface in the conventional bearing is [28]:

$$\overline{F}_{f,a}=\frac{1}{k}\left[2\ln\frac{1}{H_i}+6Q_{v,conv}\left(\frac{1}{H_i}-1\right)\right] \quad (45)$$

The dimensionless friction force per unit contact length on the moving surface in the conventional bearing is [28]:

$$\overline{F}_{fb} = \frac{1}{k}\left[4\ln H_i + 6Q_{v,conv}\left(1-\frac{1}{H_i}\right)\right] \quad (46)$$

The friction coefficients on the stationary and moving surfaces in the conventional bearing are respectively:

$$f_{a,conv} = \frac{\left|\overline{F}_{fa}\right|}{W_{conv}}, f_{b,conv} = \frac{\left|\overline{F}_{fb}\right|}{W_{conv}} \quad (47)$$

5. RESULTS

The calculations were made for the typical case $\alpha = 2.5\times10^{-4}$ and $\overline{\tau}_{sa} = 0.1$ for widely varying operational parameter values. The obtained results are discussed as follows.

5.1. Film Pressure Distribution

Figure **2** shows the dimensionless film pressure distributions in the present bearing for different λ_τ when $\psi = 0.6$ and $\theta = 1.0\times10^{-3o}$. They are compared with the dimensionless film pressures (P_{conv}) calculated from the conventional hydrodynamic lubrication theory for the same operating conditions. The pressure in the present bearing is much higher than that in the conventional mode of the bearing for the same case; Also, it is significantly increased with the increase of λ_τ .

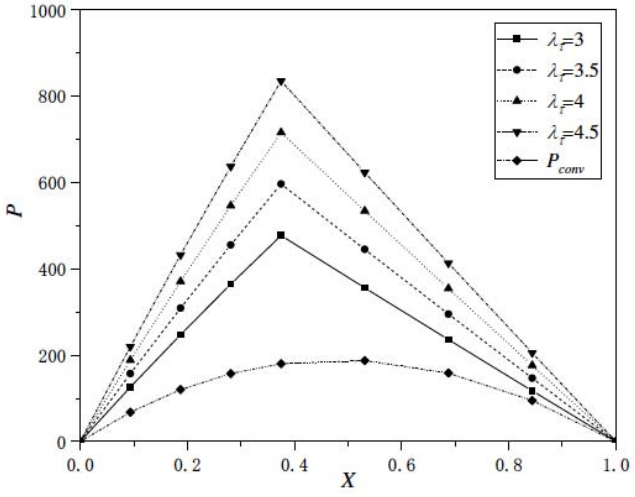

Figure 2: Dimensionless film pressure distributions in the present bearing and their comparisons with that calculated from the conventional hydrodynamic lubrication theory when $\psi = 0.6$ and $\theta = 1.0\times10^{-3o}$.

5.2. Carried Load of the Bearing

Figure **3a** shows the dimensionless carried loads of the present bearing for different θ and λ_τ when $\psi = 0.6$. They are compared with those (W_{conv}) calculated from the conventional hydrodynamic lubrication theory for the same cases. The carried load of the present bearing is much greater than that of the conventional mode of the bearing for the same case; It is slightly increased with the increase of θ ; However, it is significantly increased with the increase of λ_τ .

Figure **3b** shows that the carried load of the present bearing is linearly increased with the increase of λ_τ in the slope nearly independent on the wedge angle θ . Figure **3c** shows that the carried load of the present bearing is significantly reduced with the increase of ψ .

5.3. Friction Coefficients

Figures **4a** and **b** show that the friction coefficients f_a and f_b on the upper and lower contact surfaces in the present bearing are much lower than those ($f_{a,conv}$ and $f_{b,conv}$) in the conventional mode of the bearing for the same cases. The values of both f_a and f_b are on the scale of 0.001. The present bearing is thus obviously of low friction and energy-conserved. Both the values of f_a and f_b are significantly reduced with the increase of λ_τ , however they are almost independent on θ .

6. CONCLUSIONS

An analysis is presented for the carried load and friction coefficient of the hydrodynamic inclined fixed pad thrust slider bearing with the specially designed interfacial slippage based on the limiting interfacial shear strength model. In this bearing, the geometrical profile is normal, the interfacial slippage is designed on both the stationary surface in the inlet zone and on the whole moving surface.

The condition for the formation of the bearing was obtained. The calculation results show that the film pressure and carried load of the present bearing are much higher than those of the conventional mode of the bearing (without the interfacial slippage) for the same operating conditions; They are significantly increased with the increase of λ_τ , which is the ratio of the interfacial shear strength on the moving surface to that on the stationary surface in the inlet zone.

Compared with the conventional bearing for the same operating condition, the calculation results show that the present bearing is obviously advantageous owing to its much higher load-carrying capacity and very low friction coefficient on the scale 0.001. The

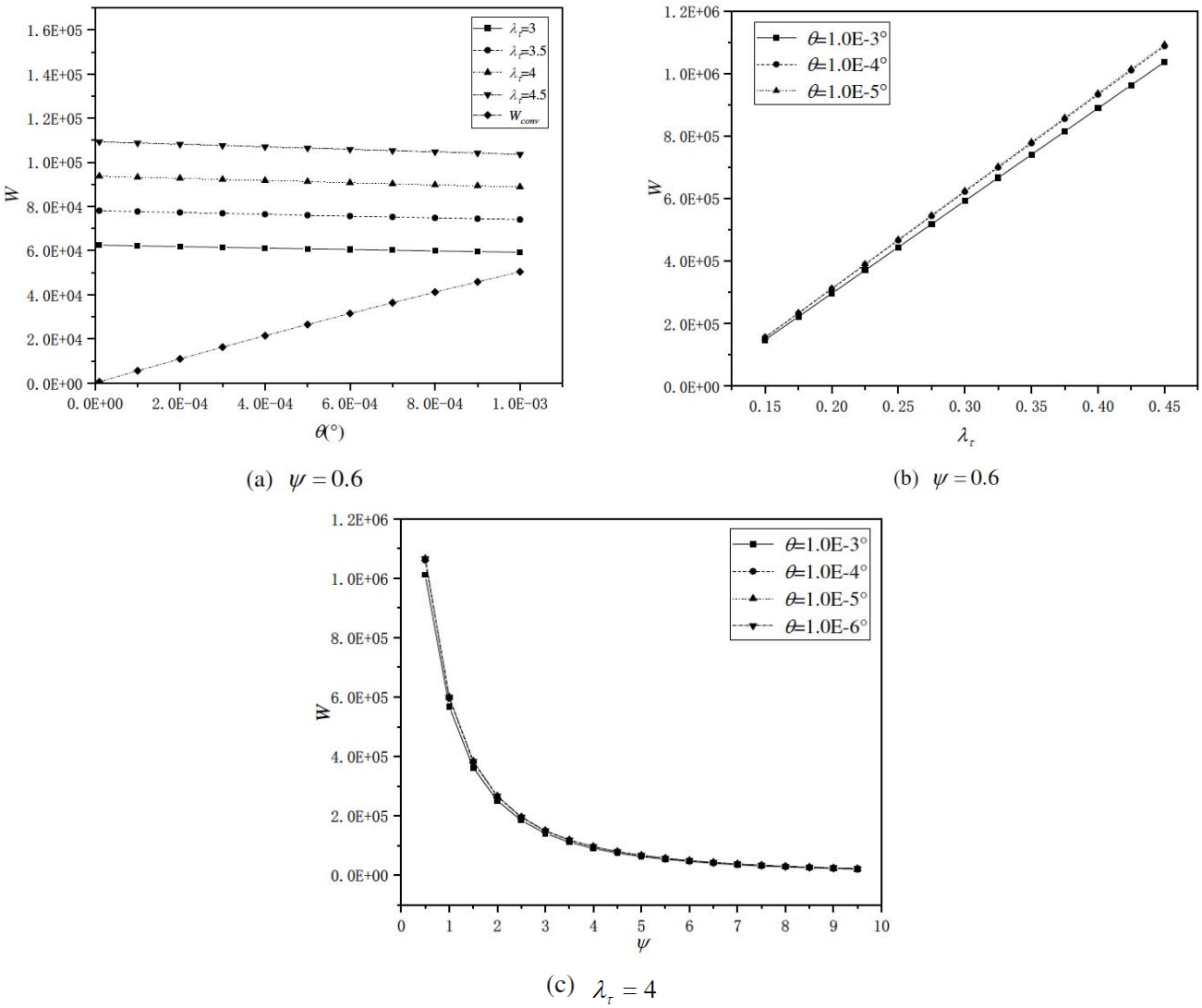

Figure 3: Dimensionless carried loads of the present bearing.

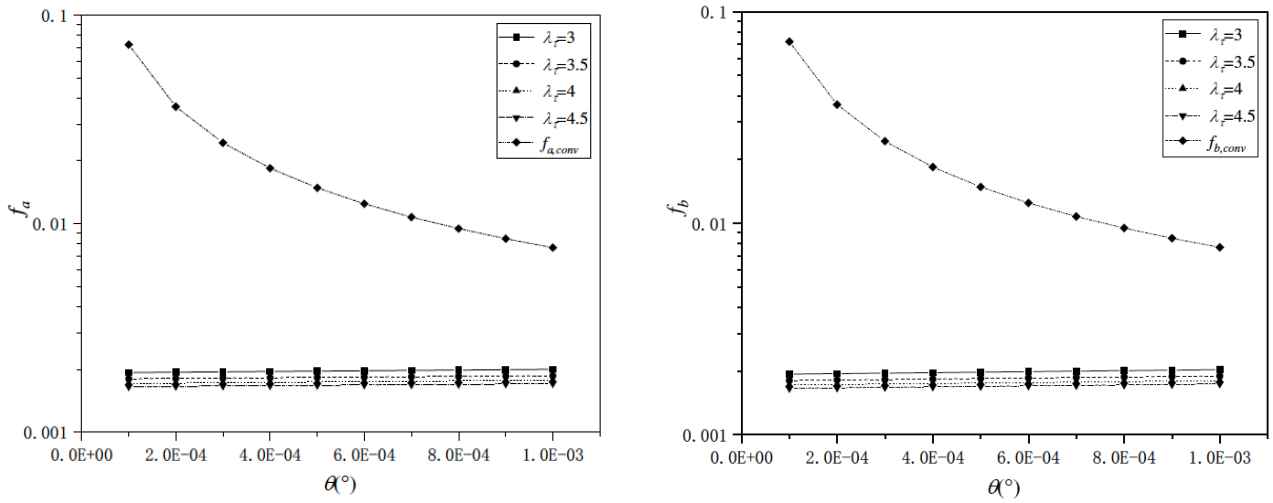

Figure 4: Friction coefficients f_a and f_b on the upper and lower contact surfaces in the present bearing and their comparisons with those ($f_{a,conv}$ and $f_{b,conv}$) calculated from the conventional hydrodynamic lubrication theory when $\psi = 0.6$.

present bearing thus has an excellent performance with significant energy conservation.

REFERENCES

[1] Liang MP, Wang JC. The inner ring of an energy conserved rolling bearing. CN201620618280.7, 2016.

[2] Hu DY. An energy conserved bearing. CN201420842351.2, 2014.

[3] Zhang KB, Fan XX. The chamber for an energy conserved bearing free of maintenance for special use in the hair-cut machine. CN200520029666.6, 2005.

[4] Li SM. The arrangements for the supporter of an energy conserved bearing for used in a ball grinding machine. CN201320592044.9, 2013.

[5] Xie ZL, Rao ZS, Na T, Liu L, Chen R. Theoretical and experimental research on the friction coefficientof water lubricated bearing with consideration of wall slip effects. Mech Ind 2016; 17: 106. https://doi.org/10.1051/meca/2015039

[6] Wu H, Zhao J, Xia W, Cheng X, He A, Yun J, Wang L, Huang H, Jiao S, Huang L, Zhang S, Jiang Z. Analysis ofTiO2 nano-additive water-based lubricants in hot rolling of microalloyed steel. J Manufactur Proc 2017; 27: 26-36. https://doi.org/10.1016/j.jmapro.2017.03.011

[7] Fortier AE, Salant RF. Numerical analysis of a journal bearing with a heterogeneous slip/no-slip surface. ASME J Trib 2005; 127; 820-825. https://doi.org/10.1115/1.2033897

[8] Salant RF, Fortier AE. Numerical analysis of a slider bearing with a heterogeneous slip/no-slip surface. Trib Trans 2004; 47: 328-334. https://doi.org/10.1080/05698190490455348

[9] Zhang YB. A tilted pad thrust slider bearing improved by the boundary slippage. Meccanica 2013; 48: 769-781. https://doi.org/10.1007/s11012-012-9630-6

[10] Zhang YB. An improved hydrodynamic journal bearing with the boundary slippage. Meccanica 2015; 50: 25-38. https://doi.org/10.1007/s11012-014-0064-1

[11] Zhang YB. Recent patents on energy conservation in gears and bearings by the boundary slippage technology. Recent Patent Mech Eng 2015; 8: 33-37. https://doi.org/10.2174/2212797608666150123002309

[12] Zhang YB. An energy conserved hydrodynamic journal bearing by the boundary slippage technology. Recent Paten Mech Eng 2016; 9: 63-70. https://doi.org/10.2174/2212797609666160118234638

[13] Zhang YB. Boundary slippage for generating hydrodynamic load-carrying capacity. Appl Math Mech 2008; 29: 1155-1164. https://doi.org/10.1007/s10483-008-0905-y

[14] Zhang YB. A concentric hydrodynamic journal bearing constructed by the boundary slippage. J Theor Appl Mech Warsaw 2016; 54: 345-352. https://doi.org/10.15632/jtam-pl.54.2.345

[15] Wang JY, Zhang YB, Pan LZ, Dong YW, Tang ZP. Abnormal hydrodynamic step bearing formed by boundary slippage. J Balkan Trib Assoc 2018; 24: 75-85.

[16] Cheng HS, Zhang YB, Tang ZP, Dong YW, Pan LZ. Abnormal hydrodynamic inclined fixed pad thrust slider bearing formed by boundary slippage. J Balkan Trib Assoc 2018; 24: 64-74.

[17] Xia Y, Zhang YB, Sun ZY, Jiang XD, Dong YW, Wang Y. Normal geometrical hydrodynamic wedge-platform thrust slider bearing with the interfacial slippage occurring on the whole stationary surface. J Balkan Trib Assoc 2020; 26: 147-162.

[18] Zhou Y, Zhang YB, Dong YW, Jiang XD, Wang Y. Performance of normal geometrical hydrodynamic step bearing with the interfacial slippage occurring on the whole stationary surface. J Balkan Trib Assoc 2019; Ms. No. 2339/14.06.2019, revised.

[19] Xia YT, Zhang YB, Wang Y, Jiang XD, Dong YW. Hydrodynamic wedge-platform thrust slider bearing with the interfaical slippage on the whole moving surface. J Balkan Trib Assoc 2019; 25: 372-382.

[20] Xia YT, Zhang YB. Performance of the hydrodynamic wedge-platform thrust slider bearing with the interfacial slippage occurring on the stationary surface in the inlet zone and on the whole moving surface. J Balkan Trib. Assoc 2020; Ms. No. 2374/04.02.2020, revised.

[21] Zhang YB. Review of hydrodynamic lubrication with interfacial slippage. J Balkan Trib Assoc 2014; 20: 522-538.

[22] Rozeanu L, Tipei N. Slippage phenomena at the interface between the adsorbed layer and the bulk of the lubricant: Theory and experiment. Wear 1980; 64: 245-257. https://doi.org/10.1016/0043-1648(80)90131-3

[23] Jacobson BO, Hamrock BJ. Non-Newtonian fluid model incorporated into elastohydrodynamic lubrication of rectangular contacts. ASME J Trib 1984; 106: 275-284. https://doi.org/10.1115/1.3260901

[24] Zhang YB. Contact-fluid interfacial shear strength and its critical importance in elastohydrodynamic lubrication. Industr Lubri Trib 2006; 58: 4-14. https://doi.org/10.1108/00368790610640064

[25] Zhang YB. A molecular calculation of the solid-liquid interfacial shear strength for low liquid pressures by using the Lennard-Jones potential model. J Balkan Trib Assoc 2014; 20: 618-629.

[26] Zhang YB. A molecular calculation of the solid-liquid interfacial shear strength for low liquid pressures by using the Coulomb interaction model. J Balkan Trib Assoc 2015; 21: 594-605.

[27] Zhang YB. Varying parametric study of the solid-liquid interfacial shear strength for low liquid pressures by using the Lennard-Jones potential model. J Balkan Trib Assoc 2014; 20: 630-638.

[28] Pinkus O, Sternlicht B. Theory of hydrodynamic lubrication, McGraw-Hill, New York 1961.

Received on 17-09-2020 Accepted on 25-10-2020 Published on 09-11-2020

DOI: https://doi.org/10.31875/2409-9848.2020.07.4